Second Order Statistics of NLOS Indoor MIMO Channels Based on 5.2 GHz Measurements

Kai Yu[1], Mats Bengtsson[1], Björn Ottersten[1], Darren McNamara[2], Peter Karlsson[3] and Mark Beach[2]
[1]Department of Signals, Sensors and Systems,
Royal Institute of Technology, Stockholm, Sweden
email: kaiyu@s3.kth.se

[2]Center for Communication Research
University of Bristol, United Kingdom

[3]Telia Research AB, Malmö, Sweden

Abstract – Herein, results from measurements conducted by the University of Bristol are presented. The channel characteristics of Multiple Input Multiple Output (MIMO) indoor systems at 5.2 GHz are studied. Our investigation shows that the envelope of the channel for non-line-of-sight (NLOS) indoor situations are approximately Rayleigh distributed and consequently we focus on a statistical description of the first and second order moments of the narrowband MIMO channel. Furthermore, it is shown that for NLOS indoor scenarios, the MIMO channel covariance matrix can be well approximated by a Kronecker product of the covariance matrices describing the correlation at the transmitter and receiver side respectively. A statistical narrowband model for the NLOS indoor MIMO channel based on this covariance structure is presented.

I. INTRODUCTION

It is well known that using antenna arrays at both the transmitter and receiver over a MIMO channel can provide very high channel capacity as long as the environment has sufficiently rich scattering. Under these circumstances, the channel matrix elements have low correlation leading to channel realizations of high rank and consequently provide substantial channel capacity increases. In [1] and [2] the channel capacity for MIMO systems has been investigated theoretically. Some experimental investigations have also been carried out trying to characterize the MIMO channel and the corresponding capacity, see [3, 4, 5, 6, 7].

There is of course great interest in modeling of MIMO channels. A so-called one-ring model has been proposed and investigated in [8]. In [9], a distributed scattering model has been proposed in order to explain the *pinhole* phenomenon that may appear in outdoor situations. In [10], a model based on channel power correlation coefficients is presented. However, models based on experimental data are still rare. In [11], the initial results for the NLOS MIMO channel measurements have been reported.

This paper reports the results based on data measured in University of Bristol as part of the SATURN project. An initial statistical model based on the experimental data is also presented. This paper is organized as follows: Section II gives a brief description of the measurement setup including the test environment and the test equipment. In Section III, a statistical structure is proposed and a least squares rank one approximation method is described in order to separate a matrix into the Kronecker product of two sub-matrices. Section IV presents a statistical model based on this covariance structure and the results from the model identification for different transmitter locations. Finally we draw some conclusions in Section V.

II. MEASUREMENT SYSTEM

The test site is the Merchant Venture's Building of the University of Bristol. The general layout of the test site includes office rooms, computer labs, corridors and open spaces. The entire measurements include 15 transmitter locations and 3 receiver locations. Both line-of-sight (LOS) and NLOS cases were measured. Notice that in this paper, all the results are from NLOS cases as shown in Fig. 1. Here, the arrow at each transmitter location indicates the orientation of the transmit array. The transmitter was located in a computer lab and the receiver was located in a large modern office with cubicles.

The measurements were carried out using the Medav RUSK BRI vector sounder, which has an 8-element omnidirectional

This work is conducted in part within SATURN (Smart Antenna Technology in Universal bRoadband wireless Networks) funded by the EU IST program.

0-7803-7206-9/01/$17.00 © 2001 IEEE

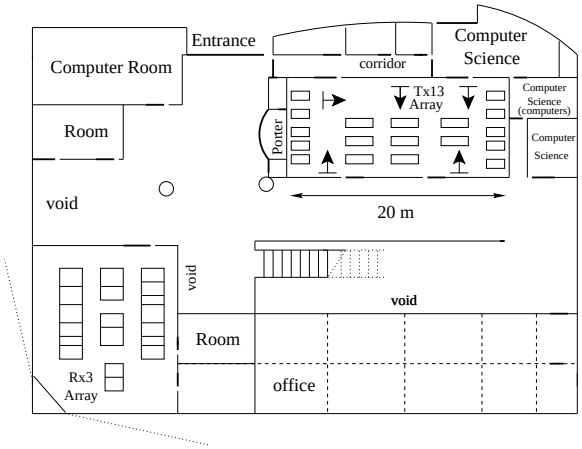

Figure 1. Measurement scenario for NLOS indoor MIMO channel

uniform linear array (ULA) at the transmitter side and an 8-element ULA with 120° beamwidth at the receiver side (for pictures, see [7]). The distance between two neighboring antenna elements is 0.5λ for both arrays. There is a feedback from the receiver to the transmitter by a cable in order to synchronize the transmitter and receiver.

The measurements were centered at 5.2 GHz. A periodic multifrequency signal with 120 MHz bandwidth was sent out by the transmitter and captured by the receiver. The channel impulse response was then sampled and saved in the frequency domain. The maximum expected channel excess delay was $0.8\mu s$, corresponding to 97 frequency subchannels. For each transmit element, one 'vector snapshot' (one measurement from each receive element) is taken by the receiver through switching control circuits. The sampling time for one MIMO snapshot (8 vector snapshots) is $102.4\mu s$, which is well within the coherence time. One complete measurement includes 199 blocks with 16 MIMO snapshots within each block, therefore there are 3184 complete MIMO snapshots in total for each frequency subchannel. The time delay between two neighboring blocks is $26.624ms$. This means the total time for one complete measurement is $5.3s$. During the measurements, people were moving around both at the transmitter and receiver side.

III. Measurement Analysis Method

A. Data Model and Second Order Statistics

Assume there are m transmit elements and n receive elements. For a narrowband MIMO channel, the input-output relationship could be expressed in the baseband as

$$\mathbf{y}(t) = \mathbf{H}_n^m \mathbf{s}(t) + \mathbf{n}(t), \tag{1}$$

where $\mathbf{s}(t)$ is the transmitted signal, $\mathbf{y}(t)$ is the received signal and $\mathbf{n}(t)$ is additive white Gaussian noise. The channel matrix $\mathbf{H}_n^m$ here is an n by m matrix.

We define the transmitter, receiver and channel covariance matrices as

$$\mathbf{R}_H^{Tx} = \mathrm{E}[(\mathbf{h}_i^* \mathbf{h}_i)^T] \quad \text{for } i = 1, \ldots, n \tag{2}$$

$$\mathbf{R}_H^{Rx} = \mathrm{E}[\mathbf{h}^j \mathbf{h}^{j*}] \quad \text{for } j = 1, \ldots, m \tag{3}$$

$$\mathbf{R}_H = \mathrm{E}[\mathrm{vec}(\mathbf{H}_n^m)\mathrm{vec}(\mathbf{H}_n^m)^*], \tag{4}$$

where

$$\mathrm{vec}(\mathbf{H}_n^m) = [(\mathbf{h}^1)^T, (\mathbf{h}^2)^T, \ldots, (\mathbf{h}^m)^T]^T, \tag{5}$$

$\mathbf{h}_i$ is ith row of $\mathbf{H}_n^m$, $\mathbf{h}^j$ is jth columns of $\mathbf{H}_n^m$, $(\cdot)^*$ is complex conjugate transpose, $(\cdot)^T$ is transpose and E[·] denotes the expected value.

In [10], it is claimed that the correlation between the power of two subchannels could be modeled by the product of the correlations seen from the transmitter and receiver. Here we try to verify whether this structure could be extended to describe also the phase of the complex valued amplitudes. Notice that for the normalized channel matrix $\mathbf{H}_n^m$, this structure can also be expressed as

$$\mathbf{R}_H = \mathbf{R}_H^{Tx} \otimes \mathbf{R}_H^{Rx}, \tag{6}$$

where $\mathbf{R}_H$ is the channel covariance matrix, $\mathbf{R}_H^{Tx}$ and $\mathbf{R}_H^{Rx}$ are the covariance matrices at the transmitter and receiver side defined in (4), (2), (3) respectively and '$\otimes$' denotes the Kronecker product.

B. Normalization Method

It is well known that when the transmitted power is equally allocated to each transmit element, the channel capacity may be expressed as in [2]

$$C = \log_2 \det(\mathbf{I}_n + \frac{\rho}{m}\mathbf{H}\mathbf{H}^*), \tag{7}$$

where $\mathbf{H}$ is the normalized channel matrix and ρ is the average signal-to-noise-ratio (SNR) at each receiver branch. To normalize the channel matrix from data, we use the same normalization factor for all realizations such that

$$\frac{1}{N}\sum_{i=1}^{N} \| \mathbf{H}_i \|_F^2 = nm, \tag{8}$$

where $\| \cdot \|_F$ denotes the Frobenius norm.

C. Least Squares Kronecker Factorization

Fitting the channel covariance matrix $\mathbf{R}_H$ optimally into the Kronecker product of two Hermitian matrices $\mathbf{X}$ and $\mathbf{Y}$ boils down to solving the following problem

$$\min_{\mathbf{X},\mathbf{Y}} \parallel \mathbf{R}_H - \mathbf{X} \otimes \mathbf{Y} \parallel_F . \tag{9}$$

The least squares rank one approximation method in [12] can be used to solve this problem. The main idea is to rearrange the elements of the covariance matrix, $\mathbf{R}_H$, and $\mathbf{X} \otimes \mathbf{Y}$ to get a least squares problem of the form

$$\min \parallel \mathbf{R}_{\text{tran}} - \mathbf{x}(\mathbf{y}^c)^* \parallel_F, \tag{10}$$

where

$$\mathbf{x} = \text{vec}(\mathbf{X}), \tag{11}$$

$$\mathbf{y} = \text{vec}(\mathbf{Y}), \tag{12}$$

$(\cdot)^c$ means complex conjugate and $\mathbf{R}_{\text{tran}}$ is the transformed matrix. To obtain the transformed matrix $\mathbf{R}_{\text{tran}}$, we use the permutation matrix $\mathbf{T}$, defined such that

$$\mathbf{T}\,\text{vec}(\mathbf{X} \otimes \mathbf{Y}) = \text{vec}(\mathbf{x}\mathbf{y}^T) \tag{13}$$

for all matrices $\mathbf{X}$ and $\mathbf{Y}$. The matrix $\mathbf{R}_{\text{tran}}$ is then defined by

$$\text{vec}(\mathbf{R}_{\text{tran}}) = \mathbf{T}\,\text{vec}(\mathbf{R}_H). \tag{14}$$

Note that (9) and (10) are equivalent since $\mathbf{T}$ is orthonormal.

The solution to the least squares rank one approximation of $\mathbf{R}_H$ in (10) is easily calculated using the singular value decomposition (SVD) [13]. Let $\lambda_{\max}$ as the largest singular value of $\mathbf{R}_{\text{tran}}$, and $\mathbf{u}_{\max}$ and $\mathbf{v}_{\max}$ as the left and right singular vector corresponding to $\lambda_{\max}$. Then, $\mathbf{x}$ and $\mathbf{y}$ can be expressed as

$$\mathbf{x} = \gamma \mathbf{u}_{\max}, \tag{15}$$

$$\mathbf{y}^c = \gamma^{-1} \lambda_{\max} \mathbf{v}_{\max}, \tag{16}$$

where γ is an arbitrary scalar and its value depends on what $\mathbf{X}$ and $\mathbf{Y}$ should be. Then it is straightforward to transform the two vectors $\mathbf{x}$ and $\mathbf{y}^c$ into $\mathbf{X}$ and $\mathbf{Y}$ inversely.

It can be shown that the solution $\mathbf{X}$ and $\mathbf{Y}$ will always be Hermitian as long as $\mathbf{R}_H$ is Hermitian, therefore it is not necessary to force that structure on the solution explicitly.

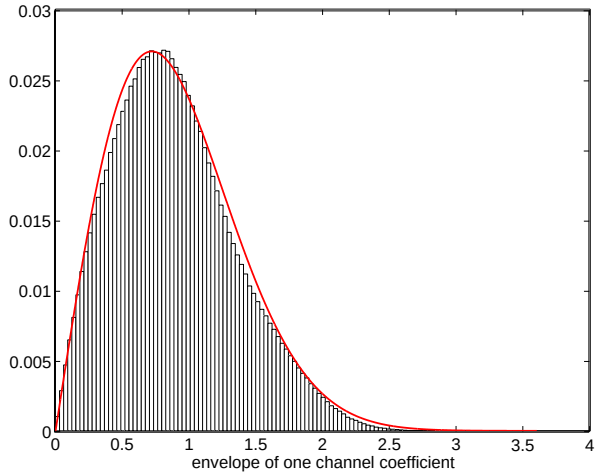

Figure 2. Histogram of the envelope of one channel coefficient for NLOS indoor MIMO scenario, Tx13-Rx3 and the fitted Rayleigh distribution envelope (normalized)

IV. Measurement Results

As stated in section II, the measurements use an 8-element transmitter and receiver. In this paper, pairs of 2 and 3 neighboring elements at both the transmitter and receiver have been used as an example to get 2x2 and 3x3 MIMO channel realizations that are used to analyze the second order statistics of the channel matrix. It is interesting to find that even though people were moving around during the measurements, the time variations on a single link of each narrowband subchannel are still not enough to give an average of zero, indicating a quite stationary scenario. Therefore both the frequency and spatial domain have been averaged, i.e. all the snapshots from different frequency subchannels and spatial 2x2/3x3 pairs (at the same Tx and Rx locations) have been seen as different channel realizations in order to get sufficient data to study both the channel distribution and second order statistics. Reasonably good results have been found for other setups with up to 5 elements at each side. The data are not enough to calculate setups with more elements due to the insufficient spatial average. In the following section, the data measured at Tx13 – Rx3 are used, see Fig. 1. Similar results have been found in the other four transmitter locations, see Fig. 1.

A. Distribution of the channel coefficient

The distribution of the channel coefficient has been investigated by plotting the histogram of the envelope of one channel coefficient and the cumulative density function (CDF) of the phase of one channel coefficient. Fig. 2 and Fig. 3 shows the

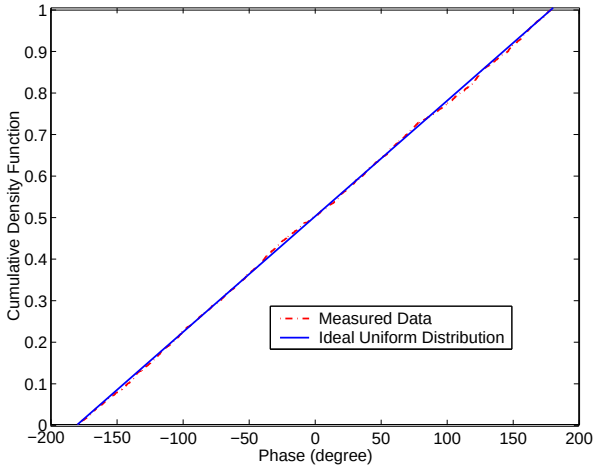

Figure 3. CDF of the phase of one channel coefficient and the CDF of the uniform distribution within [-180°,180°]

result of the envelope distribution of one channel coefficient and the CDF of the phase of one channel coefficient comparing with the fitted Rayleigh distribution and uniform distribution on $[-\pi, \pi]$ respectively. We concluded that the channel coefficient for the NLOS indoor MIMO situation is approximately zero-mean complex Gaussian.

B. *Second order statistics*

It is well known that a complex Gaussian distributed random variable is completely characterized by its first and second order moments. Although the individual elements of the channel matrix appear Gaussian distributed, we have not examined that they are jointly Gaussian. To investigate the second order statistics for this NLOS indoor scenario, we define the model error, Ψ to evaluate the difference between two matrices $\mathbf{A}$ and $\mathbf{B}$

$$\Psi(\mathbf{A}, \mathbf{B}) = \frac{\| \mathbf{A} - \mathbf{B} \|_F}{\| \mathbf{A} \|_F}. \tag{17}$$

From the measured data, two model errors have been investigated, the results are listed in the first two rows of Table 1, where the $\hat{(\cdot)}$ indicates a sample covariance estimate of the corresponding quantities in equations (2), (3), (4) respectively and the matrices $\mathbf{X}$ and $\mathbf{Y}$ are calculated using the least squares Kronecker factorization method. It is also interesting to compare the differences between the matrices $\mathbf{X}$, $\mathbf{Y}$ and the covariance matrices $\mathbf{R}_H^{Tx}$, $\mathbf{R}_H^{Rx}$ in the last two rows of Table 1. Here since γ is an arbitrary scalar, the least squares method has been used to find γ which fits all elements between two matrices.

Table 1. List of Model Errors

	2x2	3x3
$\Psi(\hat{\mathbf{R}}_H, \mathbf{X} \otimes \mathbf{Y})$	0.76 %	4.52 %
$\Psi(\hat{\mathbf{R}}_H, \hat{\mathbf{R}}_H^{Tx} \otimes \hat{\mathbf{R}}_H^{Rx})$	0.86 %	4.79 %
$\Psi(\hat{\mathbf{R}}_H^{Tx}, \mathbf{X})$	0.40 %	1.74 %
$\Psi(\hat{\mathbf{R}}_H^{Rx}, \mathbf{Y})$	0.03 %	1.60 %

From Table 1, it is clearly shown that the channel covariance matrix could be well modeled as shown in equation (6), notice that this structure could explain above 95% of the received signal power in both cases.

C. *Statistical Model and Simulations*

If the channel coefficients are complex Gaussian, it is easy to show from equation (6), as in [8], that

$$\mathbf{H} = (\mathbf{R}_H^{Rx})^{1/2} \mathbf{G} [(\mathbf{R}_H^{Tx})^{1/2}]^T, \tag{18}$$

where $\mathbf{G}$ is a stochastic M by N matrix with independent and identically distributed (IID) $\mathcal{CN}(0,1)$ elements. Here $(\cdot)^{1/2}$ denotes any matrix square root such that $\mathbf{R}^{1/2}(\mathbf{R}^{1/2})^* = \mathbf{R}$. Note that this model is also a special case of the model suggested in [9].

Monte-Carlo computer simulations have been used to generate 1000 channel realizations and the CDF of the simulated channel capacity is compared with that from the measured data. The results for the 2x2 and 3x3 cases are given in Fig. 4. As a reference, the capacity for the IID channel is also included. From the figure, it is shown that the simulated CDF fits the CDF of measured data quite well, which agrees with our model.

V. Conclusions

We access experimental MIMO channel measurements at 5.2 GHz. Our investigation shows that for NLOS indoor MIMO scenarios, the elements of the narrowband channel matrix are zero-mean complex Gaussian. Furthermore, it is shown that the channel covariance matrix can be well approximated by the Kronecker product of the covariance matrices at the transmitter and receiver side respectively. We also introduce a narrowband model for the NLOS indoor MIMO channel based on this second order statistical structure. Monte-Carlo simulations of the channel capacity have shown good agreement between the measured data and the statistical model.

References

[1] I. Emre Telatar, "Capacity of multi-antenna Gaussian channels," *European Transactions on Telecommunications*, vol. 10, no. 6, pp. 585–595, Nov./Dec. 1999.

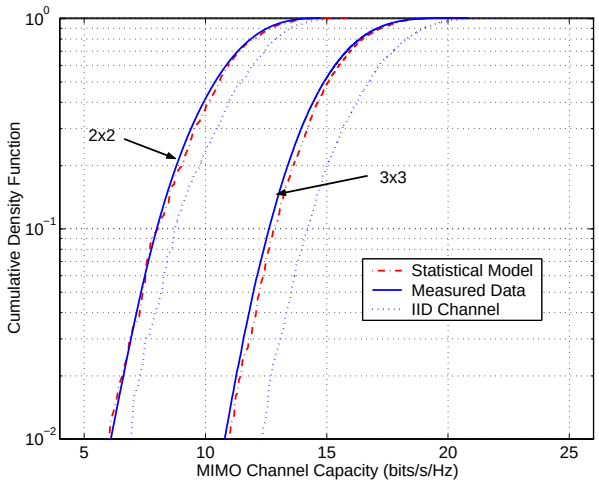

Figure 4. Cumulative density function of channel capacity for measured data, statistical model and IID MIMO channel. The SNR at the receiver side is 20dB. Power is equally allocated to the transmit elements

[2] G. J. Foschini and M. J. Gans, "On limits of wireless communications in a fading environment," *Wireless Personal Communications*, vol. 6, pp. 311–335, 1998.

[3] Jean Philippe Kermoal, Laurent Schumacher, Preben E. Mogensen, and Klaus I. Pedersen, "Experimental investigation of correlation properties of MIMO radio channels for indoor picocell scenarios," in *Proceedings IEEE Vehicular Technology Conference*. IEEE VTC Fall, 2000, pp. 14–21.

[4] Carol C. Martin, Jack H. Winters, and Nelson R. Sollenberger, "Multiple-Input-Multiple-Output (MIMO) radio channel measurements," in *Proceedings IEEE Vehicular Technology Conference*. IEEE VTC Fall, 2000, pp. 774–779.

[5] Rickard Stridh and Björn Ottersten, "Spatial characterization of indoor radio channel measurements at 5 GHz," in *Proceedings IEEE Sensor Array and Multichannel Signal Processing Workshop*, March 2000.

[6] Rickard Stridh, Peter Karlsson, and Björn Ottersten, "MIMO channel capacity on a measured indoor radio channel at 5.8 GHz," in *Proceedings of the Asilomar Conference on Signals, Systems and Computers*, October 2000.

[7] D. P. McNamara, M. A. Beach, P. N. Fletcher, and P. Karlsson, "Initial investigation of multiple-input multiple-output channels in indoor enviroments," in *Proceedings IEEE Benelux Chapter Symposium on Communications and Vehicular Technology, Leuven, Belgium*, October 2000.

[8] Da-Shan Shiu, G. J. Foschini, M. J. Gans, and J. M. Kahn, "Fading correlation and its effect on the capacity of multielement antenna systems," *IEEE Transactions on Communications*, vol. 48, no. 3, pp. 502–513, March 2000.

[9] D. Gesbert, H. Bölcskei, D. Gore, and A. Paulraj, "MIMO wireless channels: capacity and performance," in *Proceedings Global Telecommunications Conference*, November 2000, vol. 2, pp. 1083–1088.

[10] K. I. Pedersen, J. B. Andersen, J. P. Kermoal, and P. Mogensen, "A stochastic Multiple-Input-Multiple-Output radio channel model for evaluation of space -time coding algorithms," in *Proceedings IEEE Vehicular Technology Conference*. Fall, 2000, pp. 893–897.

[11] Kai Yu, Mats Bengtsson, Björn Ottersten, Peter Karlsson, Darren McNamara, and Mark Beach, "Measurement analysis of NLOS indoor MIMO channels," in *IST Mobile Communications Summit, Barcelona, Spain*, September 2001.

[12] Peter Strobach, "Low-rank detection of multichannel Gaussian signals using block matrix approximation," *IEEE Transactions on Signal Processing*, vol. 43, no. 1, pp. 233–242, January 1995.

[13] Gene H. Golub and Charles F. Van Loan, *Matrix Computations*, The Johns Hopkins University Press, London, 3rd edition, 1996.